Corrosion Behavior of Alumina-Aluminum and Silicon Carbide-Aluminum Metal-Matrix Composites

*P.C.R. Nunes and L.V. Ramanathan**

ABSTRACT

Particle-reinforced, aluminum-based metal-matrix composites (MMCs) are being considered for a range of applications. Their mechanical properties have been investigated in detail, but more information about their corrosion behavior is needed. The influences of alloy composition; particle characteristics such as composition, size, volume fraction, and pretreatment; and composite post-treatment on the aqueous corrosion behavior of aluminum-matrix composites prepared by the melt stirring process were studied. Corrosion tests consisted of prolonged immersion and anodic polarization measurements in sodium chloride (NaCl) solutions. The difference between the corrosion potential (E_{corr}) and the pitting potential (E_p) was lowered from ~ 500 mV_{SCE} in deaerated NaCl to 100 mV_{SCE} in aerated NaCl. Particle addition affected E_p but not E_{corr}. Immersion test data revealed significant specimen weight loss for the composites resulting from formation of pits or microcrevices in the matrix near the particle-matrix interface and from particle dropout. Pits in the silicon carbide (SiC) composites were deeper than those in the alumina (Al_2O_3) composites, probably because the SiC particles acted as efficient cathodic sites. Pit initiation and propagation occurred at weak spots in the air-formed film, corresponding to phase discontinuities and second-phase particles and to oxygen reduction at the particles or precipitates. Anodization and ceria (CeO_2) coatings improved corrosion resistance of the composites.

KEY WORDS: alumina, aluminum, aqueous corrosion, corrosion resistance, metal-matrix composites, particle reinforcements, phases, pitting, silicon carbide

Submitted for publication February 1994; in revised form, May 1995.

* Comissao Nacional de Energia Nuclear, Instituto de Pesquisas Energeticas e Nucleares, C.P. 11049, Cidade Universitaria, Sao Paulo, 05422-970, Brazil.

INTRODUCTION

Of the various "new" metallic materials, metal-matrix composites (MMCs) are anticipated to have a significant niche in such industries as defense, aerospace, automotive, and sports. The combination of properties such as high modulus and stiffness, low density, and reduced coefficient of thermal expansion are the main attributes of MMCs. A significant amount of data is available about their mechanical properties and about the correlations between the processing route, microstructure, and properties of MMCs.

More information concerning their corrosion behavior is needed. Corrosion behavior is associated closely with the presence of heterogeneities, and MMCs have a large quantity of heterogeneities in the form of reinforcement, microcrevices, voids, porosity, second-phase precipitates, and interaction products.

Although MMCs encompass a very wide range of matrix-reinforcement combinations, the silicon carbide-aluminum (SiC-Al) and aluminum-alumina (Al-Al_2O_3) particle combinations seem to be the most interesting for industrial applications. These composites can be produced by a variety of techniques. Although the powder metallurgy (PM) technique has been used extensively, the molten-metal process is considered the most economical for large-scale production.

Corrosion studies on SiC-Al MMCs produced by the PM route have focused on the effects of the reinforcement on pitting potential (E_p), pit morphology, and general corrosion susceptibility in chloride (Cl^-) solutions.[1-4] Trzaskoma, et al., reported that E_p values were alloy-dependent, rather than reinforce-

0010-9312/95/000137/$5.00+$0.50/0

TABLE 1
Al-7.5% Si-1% Mg Alloy Composites Designation and Characteristics

Designation[A]	Reinforcement			
	Type	Vol%	Size (μm)	Treatment
CA-05-20	Al_2O_3	5	20	–
CA-05-100	Al_2O_3	5	100	–
CA-20-100	Al_2O_3	20	100	–
CC-05-50	SiC	5	50	–
CC-10-50	SiC	10	50	–
CC-05-100	SiC	5	100	–
CC-10-100	SiC	10	100	–
COC-05-50	SiC	5	50	Oxidized

[A] CA = composite with Al_2O_3, CC = composite with SiC, and COC = composite with preoxidized SiC.

ment-dependent.[1] It was shown that more pits formed in composite materials than in the unreinforced matrix alloy.[1,5-8] Corrosion tests carried out with squeeze-cast aluminum composites also showed composites corroded faster.[9] Among the composites tested, those reinforced with fibers corroded faster than the particulate composites.[9] Paciej and Agarwala investigated the effects of powder processing Aluminum Association (AA)[1] alloy 7091 (UNS A97091)[2] and SiC composites and found that a high extrusion ratio and modified solution heat treatment, which affected precipitation behavior, enhanced the corrosion resistance.[10] Bhat, et al., also reported that extruded SiC particulate (SiCp)-AA 6061 (UNS A96061) composites corroded less than the unextruded composites, which they attributed to the presence of fewer pores.[8] McIntyre, et al., reported that the precipitation behavior and, consequently, the pitting susceptibility of heat-treatable matrix alloys varied in the presence of SiC particles.[11-12]

Microstructural changes at the matrix-reinforcement interface have been shown to affect the mechanical behavior of MMCs.[13] These changes can result from one or more of the following: the matrix alloy, the particle surface characteristics, the processing route, and/or the subsequent heat treatment. The influences of some of these parameters on the corrosion behavior of PM-processed MMCs have been reported.[7,14] The effect of surface treatments such as anodization and the formation of cerium oxide (CeO_2) films upon immersion in cerium chloride ($CeCl_2$) solution on the corrosion behavior of aluminum-based alloys and composites has been studied, and improvements to corrosion resistance have been reported.[1,15-17]

The objective of the present work was to study the effects of particle characteristics such as composition, SiC volume fraction, and pretreatment; matrix alloy composition; and MMC surface treatments, such as anodization and application of CeO_2 films, on the aqueous corrosion behavior of aluminum-matrix composites.

MATERIALS AND METHODS

Al-7.5% Si-1% Mg and AA 2014 (UNS A92014, Al-4.5% Cu-1% Si-0.8% Mn-0.5% Mg) were used to prepare the MMCs. The composite preparation procedure consisted of adding preheated (and pretreated where relevant) particles of either SiC or Al_2O_3 to a vigorously stirred bath of the molten alloy. After 10 min of agitation, the composites were poured into chilled copper molds and allowed to solidify. Particles of varying size were used, and composites with different particle volume fractions were prepared. Composites also were prepared with preoxidized SiC particles. The preoxidation was carried out at 1,100°C for 2 h in air to form a 50-nm layer of silicon dioxide (SiO_2) on the SiC particles.[18] The composite processing parameters (i.e., melt temperature, stirrer design, stirring rate, and duration) that affected reinforcement distribution were maintained at their optimized values to obtain uniform particle distribution.[19] Table 1 summarizes the different composites and their characteristics. The MMC surface treatment consisted of anodization in 16 wt% sulfuric acid (H_2SO_4) at 23°C at 27 mA/cm^2 (18 V) for 30 min followed by sealing in boiling water for 30 min and then immersion in concentrated $CeCl_2$ for 100 h followed by rinsing. Specimens 10 mm by 10 mm by 3 mm (0.394 in. by 0.394 in. by 0.118 in.) were cut from the as-cast and the surface-treated composites for corrosion measurements.

The corrosion measurements consisted of anodic potentiodynamic polarization in 3.5% sodium chloride (NaCl) and immersion testing in 3.5% NaCl at 25°C for 28 days. Specimens for the electrochemical measurements were cut to 5 mm by 5 mm by 3 mm (0.197 in. by 0.197 in. by 0.118 in.), mounted in

[1] Aluminum Association, 900 19th St., N.W., Suite 300, Washington, DC, 20006.
[2] UNS numbers are listed in *Metals and Alloys in the Unified Numbering System*, published by the Society of Automotive Engineers (SAE) and cosponsored by ASTM.

TABLE 2
Average Corrosion Weight Loss in 3.5% NaCl, pH 7.0, After 28 Days

Specimen[A]	Weight Loss (mdd)	
	Overall	Corrected
CC-05-20	2.37	1.42
CC-05-50	3.41	2.05
CC-05-100	5.6	3.36
CC-10-50	4.67	2.80
CC-10-100	6.12	3.67
COC-05-50	5.58	3.35
CA-05-20	4.75	2.85
CA-05-50	6.95	4.17
CA-05-100	4.45	2.67
CA-10-50	4.61	2.77
CA-10-100	4.38	2.63

[A] CA = composite with Al_2O_3, CC = composite with SiC, and COC = composite with preoxidized SiC.

epoxy, ground to 600 grit, rinsed in deionized water, and introduced into a standard corrosion cell. The specimens were allowed to equilibrate prior to measurement of their corrosion potential (E_{corr}) and before initiation of anodic scans from –1,400 mV_{SCE} to 100 mV_{SCE} at 10 mV/s. The potential-vs-current curves were recorded.

Measurements were carried out in aerated and deaerated NaCl. Deaeration was achieved by bubbling nitrogen gas (N_2) through the electrolyte before and during the measurements. Specimens for the immersion tests (10 mm by 10 mm by 3 mm [0.394 in. by 0.394 in. by 0.118 in.]) were prepared by grinding to 600 grit, degreasing, and rinsing. The specimens were suspended in 3.5 wt% NaCl maintained at 25°C at pH 7. After the test, the specimens were cleaned in 50 vol% nitric acid (HNO_3), dried, and weighed. The weight-loss values resulting from corrosion of the matrix and particle dropout are given as overall weight loss in Table 2.

A series of parallel experiments were carried out with the matrix alloy and some composites to determine the average weight loss due to particle dropout. In these experiments, small beakers were positioned within the testing tank of NaCl to collect the dislodged particles. At the end of the test, the specimens were cleaned with 10% HNO_3 and rinsed in a manner to permit the particles and the corrosion products to be collected. The solution containing the particles and the corrosion products were filtered, and the weight of the residue was determined. The overall percent contribution of the reinforcement and intermetallic precipitates in the residue weight was found to be ~ 40%. Based on this, the corrected corrosion weight-loss values for the composites were determined and are given in Table 2. In tests carried out to study pit morphology, specimens were exposed to 3.5% NaCl at 10 mV > E_p for different durations. The specimens were rinsed thoroughly and examined by scanning electron microscopy (SEM) using analytical attachments.

RESULTS

Microstructure

The as-cast microstructures of Al-7.5% Si-1% Mg, its alumina composite, and alloy AA 2014 are shown in Figures 1 and 2. In the Al-7.5% Si-1% Mg alloy, primary dendrites and eutectic Si were evident. The microstructure of as-cast AA 2014 (Figure 2) was obtained by etching the polished specimen with Keller's reagent.[20] A number of light and dark particles were revealed. The light gray particles were identified by energy dispersive spectroscopy (EDS) to be cupric aluminide ($CuAl_2$). The dark particles showed weak EDS peaks of manganese, silicon, and

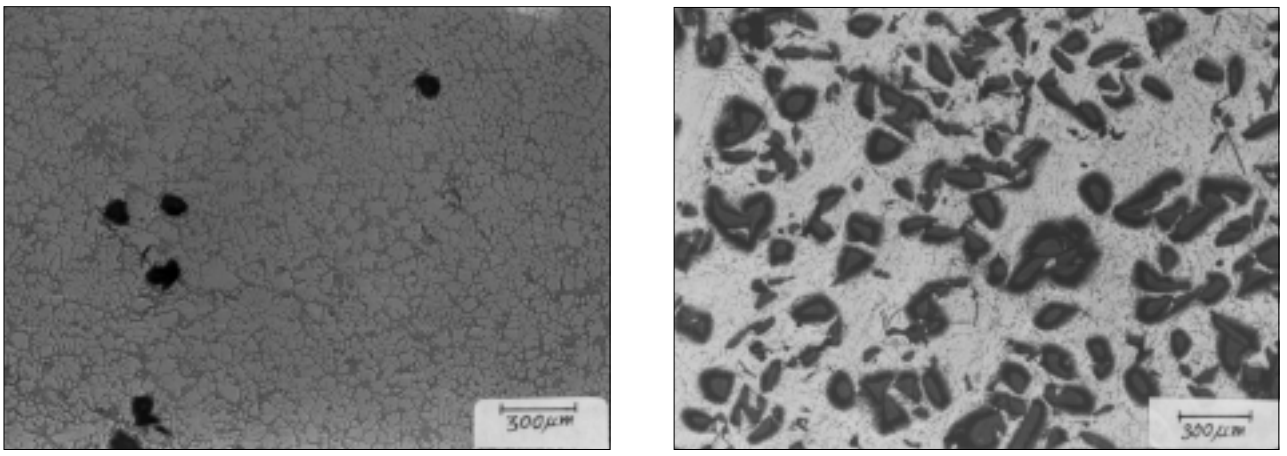

(a) (b)

FIGURE 1. *Optical micrographs of as-cast (a) Al-7.5% Si-1% Mg alloy and (b) Al_2O_3 composite.*

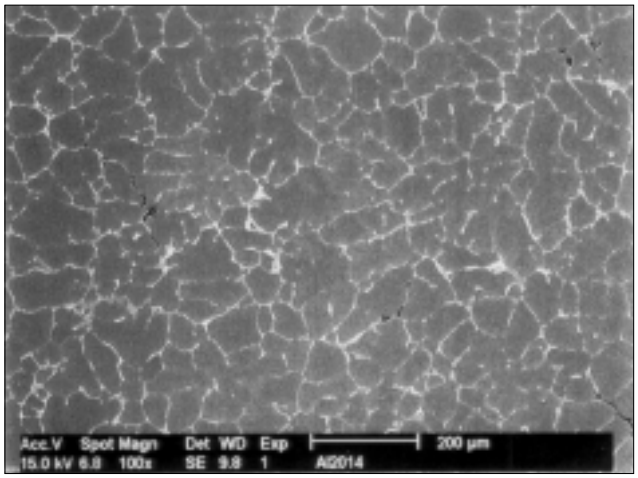

FIGURE 2. *SEM micrograph of as-cast AA 2014.*

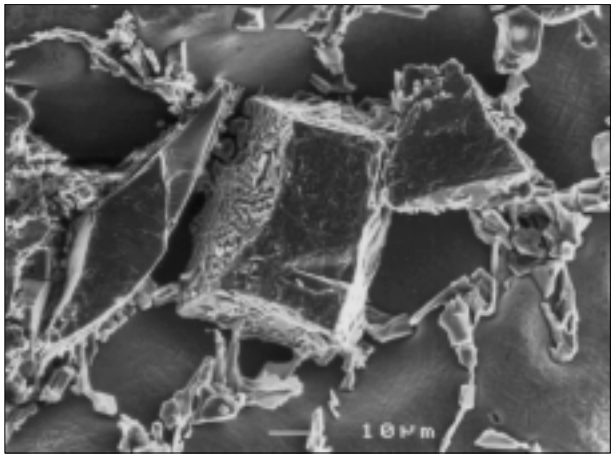

FIGURE 3. *SEM micrograph of Al-7.5% Si-1% Mg alloy/preoxidized SiC composite.*

aluminum, indicating these to be probably iron-manganese silicon aluminide ([FeMn]SiAl).[21] The reinforcement in the composites of the two alloys was distributed fairly well. Significant improvements in particle distribution were achieved by controlling the composite processing parameters. Nevertheless, particle clustering could not be eliminated completely. In composites made with preoxidized SiC other than SiC and eutectic silicon, a large number of silicon particles were observed at the SiC-matrix interface (Figure 3). This interfacial silicon was considered to result from Reaction (1), where magnesium-aluminum oxide is the other product:

$$2SiO_2 + 2Al + Mg \rightarrow MgAl_2O_4 + 2Si \quad (1)$$

Although it has been reported that this reaction is more likely to occur in aluminum alloys with low silicon and high magnesium (such as AA 6061), it also has been shown to occur in aluminum alloys with high silicon and low magnesium.[18,22] Another possible source for silicon formation at the SiC-matrix interface was Reaction (2):

$$4Al + 3SiC \rightarrow Al_4C_3 + 3Si \quad (2)$$

This reaction is unlikely to occur in aluminum alloys with high silicon, similar to those used in this investigation.[23] Also, no evidence of aluminum carbide (Al_4C_3) was observed at the interface.

Electrochemical Measurements

The anodic polarization curves of Al-7.5% Si-1% Mg, AA 2014, and the composites in aerated and deaerated NaCl solutions were found to be similar, and Figure 4 shows typical curves in aerated and deaerated NaCl. E_p, denoted by the potential at which the current increased, was read from these curves.

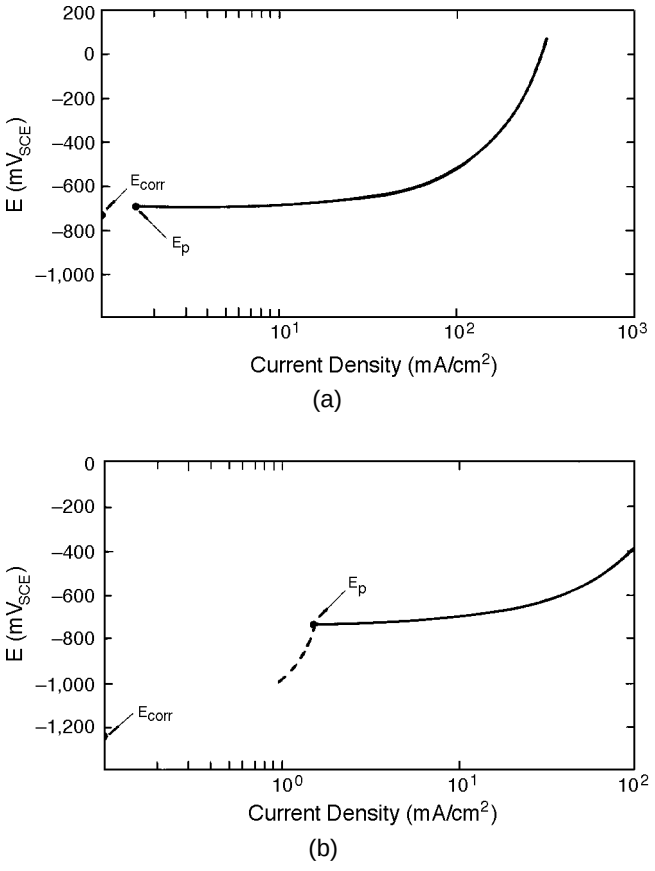

FIGURE 4. *Anodic potentiodynamic polarization curves of Al-7.5% Si-1% Mg alloy in 5% NaCl: (a) aerated and (b) deaerated.*

Table 3 lists E_p and E_{corr} values for the different specimens. In deaerated NaCl, E_p of the Al-7.5% Si-1% Mg alloy and its composites were 300 mV to 500 mV higher than their corresponding E_{corr}. This difference in potential was observed for composites containing

TABLE 3

E_{corr} and E_p of Al-7.5% Si-1% Mg Alloy and Its Composite Specimens in Aerated and Deaerated 3.5% NaCl

Specimen[A]	Aerated		Deaerated	
	E_{corr} (mV_{SCE})	E_p (mV_{SCE})	E_{corr} (mV_{SCE})	E_p (mV_{SCE})
Alloy	–760	–695	–1,140	–719
CA-05-20	–736	–608	–1,220	–688
CA-05-100	–740	–675	–1,240	–625
CA-20-100	–760	–620	1,070	–599
CC-05-50	–735	–639	1,030	–659
CC-10-50	–733	–688	1,130	–678
CC-05-100	–755	–600	–930	–713
CC-10-100	–744	–721	–1,100	–728
COC-05-50	–764	–650	–885	–746

[A] CA = composite with Al_2O_3, CC = composite with SiC, and COC = composite with preoxidized SiC.

TABLE 4

E_{corr} and E_p of Al-7.5% Si-1% Mg Alloy and AA 2014 Composites in the As-Cast, Anodized, and CeO_2-Coated Conditions in Aerated 3.5% NaCl

Specimen[A]	E_{corr} (mV_{SCE})			E_p (mV_{SCE})		
	As-Cast	Anodized	CeO_2-Coated	As-Cast	Anodized	CeO_2-Coated
Al-7.5% Si-1% Mg + CC-05-100	–755	–725	–760	–600	–458	–490
AA 2014 + CC-05-100	–700	–644	–595	–500	–440	–400

[A] CC = composite with SiC.

Al_2O_3 and composites containing SiC. Addition of SiC or Al_2O_3 particles to Al-7.5% Si-1% Mg did not alter E_{corr} in deaerated or aerated NaCl.

These observations differed from those of Maahn and Roepstorff, who reported increases in E_{corr} with the addition of SiC to SiC-Al composites.[23] In aerated NaCl, the difference between E_p and E_{corr} reduced to ~ 100 mV_{SCE}, mainly because of an increase in E_{corr} in aerated solutions. Aeration of NaCl brought about only a slight increase in E_p of the alloy and the composite. The addition of Al_2O_3 or SiC to the alloy resulted in a small increase in E_p. However, increases in particle size or quantity did not alter E_{corr} and E_p significantly. Preoxidation of SiC particles did not affect E_{corr} or E_p of the composites in aerated or deaerated solutions.

Table 4 lists E_{corr} and E_p values of the as-cast, anodized, and CeO_2-coated composites of Al-7.5% Si-1% Mg and AA 2014 in aerated NaCl. E_{corr} and E_p of alloy AA 2014 were higher than values of Al-7.5% Si-1% Mg because of the presence of Cu in the alloy.[25] Anodization of the alloys increased E_{corr} and E_p. The application of CeO_2 did not vary E_{corr} of the alloys. E_p of the anodized composite specimens and of the CeO_2-coated specimens were significantly higher than those of the as-cast composites. The increased pitting resistance of the composite specimens previously dipped in $CeCl_2$ was attributed to the formation of a defect-free durable CeO_2/cerium hydroxide ($Ce[OH]_2$) film on the surface, similar to observations made by Mansfeld, et al.,[16] and Hinton, et al.[17] Improvements in pitting resistance of anodized SiC-Al composites also have been reported elsewhere.[1]

Long-Term Immersion Tests

Overall and corrected weight-loss data for the composite specimens following 28 days of immersion in 3.5% NaCl are given in Table 2. Weight loss from corrosion was considerable in all cases. The loss was due to matrix corrosion and to particle loss originating from preferential dissolution of the interfacial regions. The weight loss of SiC-reinforced composites was found to be higher than that of the Al_2O_3-reinforced composites. This behavior was attributed to the differences in electrical conductivity of the two types of reinforcements, as well as to SiC being more noble than the matrix.[26] Preoxidation of SiC resulted in an increase in the long-term corrosion behavior, due mainly to the precipitation of silicon at the particle-matrix interface, and to differences in E_{corr} between aluminum (–0.85 V) and silicon (–0.26 V).[27]

Pit Morphology

Two sets of pit morphological studies were carried out. In the first, specimens held for 15 min at ~ 50 mV above E_p in NaCl were examined. In the second, the specimens exposed to 3.5% NaCl for 28 days were examined. The Al-7.5% Si-1% Mg alloy

exposed at a fixed potential revealed sporadic pits and pit clusters. In the composites containing Al_2O_3, microcrevice formation was observed at and in the vicinity of the interfacial regions (Figure 5[a]). The nature of the attack in both materials was similar. The microcrevice formation was more widespread in regions where Al_2O_3 particle clusters were present. At higher magnifications, crystallographic faceting also was observed in the alloy and in the composite (Figure 5[b]). The pits formed in SiC composites were deeper than those formed in Al_2O_3 composites under identical conditions (Figure 5[c]). Trzaskoma, et al., reported the formation of shallow pits in SiC-AA 6061 composites compared to those in the unreinforced alloy.[1,28] In the present investigation, however, pit sizes in SiC composites varied considerably, and crystallographic faceting was observed in both the alloy and in the composites, which was contrary to observations reported elsewhere.[29]

In the as-cast alloy exposed for 28 days, the pits were few but deep. The pits were crystallographic where inclusions were present. At higher magnifications, the matrix near the eutectic silicon near the grain boundaries was smooth and dimpled (Figure 6[a]). In AA 2014, corrosion initiated in the matrix adjacent to the more noble intergranular $CuAl_2$ (Figure 6[b]).

In the Al_2O_3 composites, preferential dissolution of the matrix around the particles led to particle dropout (Figure 7[a]). In the SiC composites, smooth hemispherical pits also were found around the particles alongside the dimpled regions (Figure 7[b]). The differences in pit morphology (i.e., crystallographic in the polarized specimens and hemispherical in specimens exposed for 28 days to NaCl) at the open-circuit potential was attributed to differences in the potential and increases in concentration of the electrolyte near the pitted surface in the immersion tests, which led to surface smoothing.[30-31]

DISCUSSION

Aluminum alloys generally pit in solutions containing Cl^-. This has been observed in unreinforced alloy as well as in the matrix of the composite. Pits initiate at flaws in the surface oxide, and these flaws often correspond to heterogeneities on the metallic surface. In the as-cast alloy or the composite, these heterogeneities were one or a combination of the following: casting defects, due mainly to solidification shrinkage and hydrogen liberation; second-phase particles or other precipitates; reinforcements; and/or reinforcement-matrix interaction products. The total number of intermetallic precipitates in the composites generally were considerably higher than in the unreinforced alloy subjected to identical treatments. Consequently, candidate sites for pit initiation in the composites were higher. The fact that

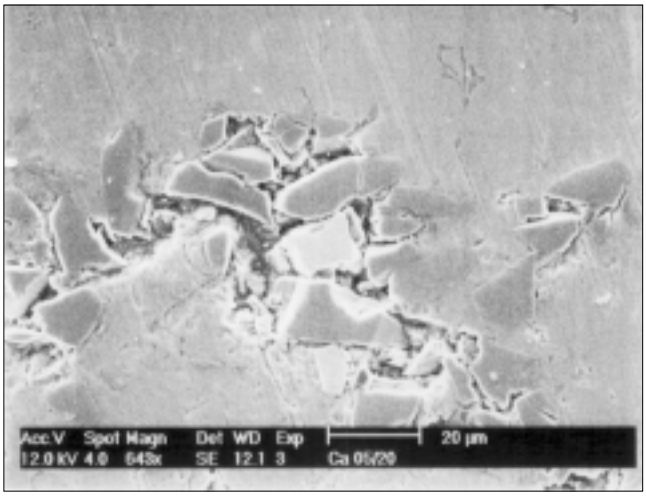

(a)

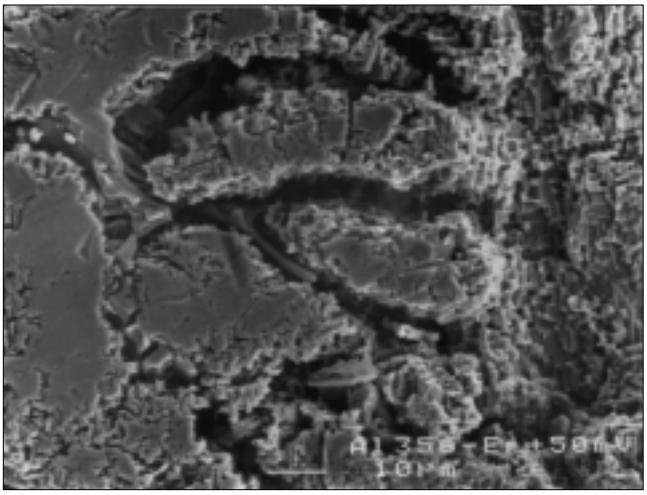

(b)

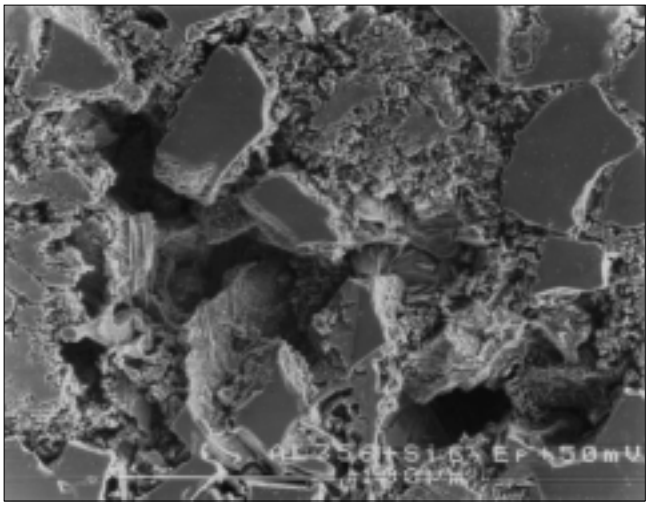

(c)

FIGURE 5. *SEM micrographs of (a): CA-05-20 composite, (b) Al-7.5% Si-1% Mg alloy, and (c) CC-05-50 composite surface exposed for 15 min at 50 mV > E_p in 3.5% NaCl. (See Table 1 for composite characteristics.)*

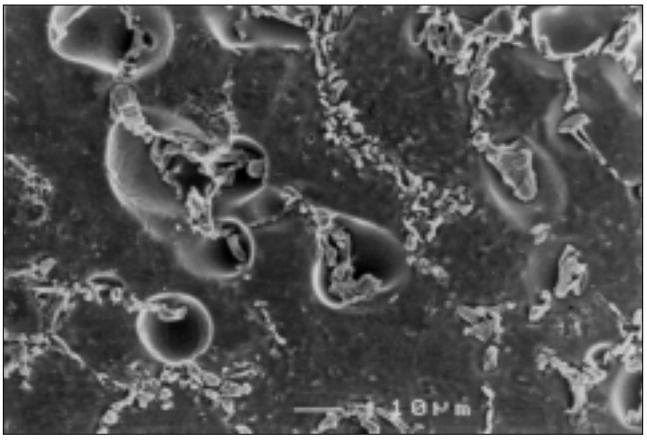

(a)

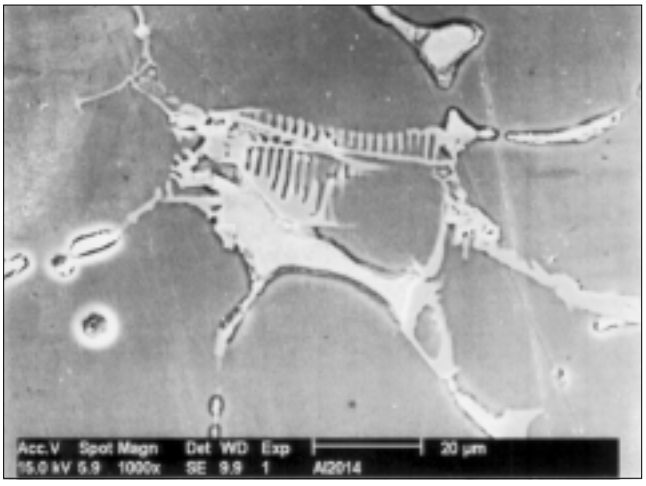

(b)

FIGURE 6. *SEM micrographs of: (a) Al-7.5% Si-1% Mg alloy and (b) AA 2014 exposed to 3.5% NaCl for 28 days.*

unreinforced and reinforced aluminum alloys pitted spontaneously in quiescent aerated solutions containing Cl^- and that E_{corr} values of the aluminum alloys were more positive in aerated than in deaerated NaCl, the primary driving force for corrosion in aerated media was the oxygen reduction reaction.[26] The cathodic sites in the unreinforced alloy were the eutectic silicon and/or the intermetallic precipitates, whereas, in the composites, depending on the composition of the alloy, the cathodic sites were the reinforcements, second-phase precipitates, or the interfacial reaction products.

Pit initiation involves the adsorption of Cl^- at the flaws in the surface oxide film, followed by chemical reaction between the Cl^- and the oxide.[31] During the pit propagation stage, direct attack of the exposed metal by Cl^- takes place. During this stage, the heterogeneity of the alloy and/or the surface assumes major importance, and the properties of the oxide film no longer govern. The electrochemical properties of the various surface phases control the overall pitting behavior.

The presence of a very large number of second-phase particles and mostly more noble eutectic silicon or SiC in the composites led to extensive pitting of the matrix and of the composites in general. Since the size of the particulate reinforcement was significantly higher than that of the precipitates, the stress state in the matrix adjoining the reinforcement (due mainly to differences in the coefficient of thermal expansion) made them conducive to dissolution and pitting.[32] A combination of the above factors resulted in increased pitting of the composite compared to the monolithic alloy.

Specific composite processing conditions also resulted in alteration of the particle-matrix interface composition and in the formation of crevices rather than pits. Similar data were reported previously.[3,33] Overall, it can be stated that the introduction of the reinforcement into the matrix alloy gave rise to two kinds of corrosion problems. The first was associated with galvanic effects. In the SiC composites, the particles and silicon were more noble. In the Al_2O_3-containing composites, galvanic coupling existed to a reduced extent between the precipitated second phases (or silicon) and the matrix. The second problem involved the formation of microcrevices at the interfaces and voids. Certain interfacial defects arose from incomplete cohesion between reinforcement and matrix. At these defects, the local chemistry necessary to retard local repassivation was achieved early and crevices or trenches formed.

In the present investigation, both forms of defects induced by particle addition were observed, either singly or jointly. Increases in corrosion resistance of the composites from anodization or immersion in $CeCl_2$ solutions were attributed to the formation of a defect-free surface film.

CONCLUSIONS

❖ In NaCl solutions, E_p values of the alloys and of the composites were not affected significantly by aeration of the solution. E_p values of the composites were slightly higher than those of the alloys in aerated NaCl. Increases in reinforcement size or volume fraction did not alter E_{corr} or E_p much.

❖ The number of pit initiation sites was significantly higher in the composites than in the alloys. The particle-matrix precipitate-matrix and eutectic silicon-matrix interfacial regions were the preferred sites for pitting and/or dissolution.

❖ The cathodic oxygen reduction reaction was considered to be the main driving force for the corrosion process, and the SiC particles, eutectic silicon, and the precipitated phases were the cathodic sites in the Al-7.5% Si-1% Mg composites. In AA 2014 composites, $CuAl_2$ were the preferred sites.

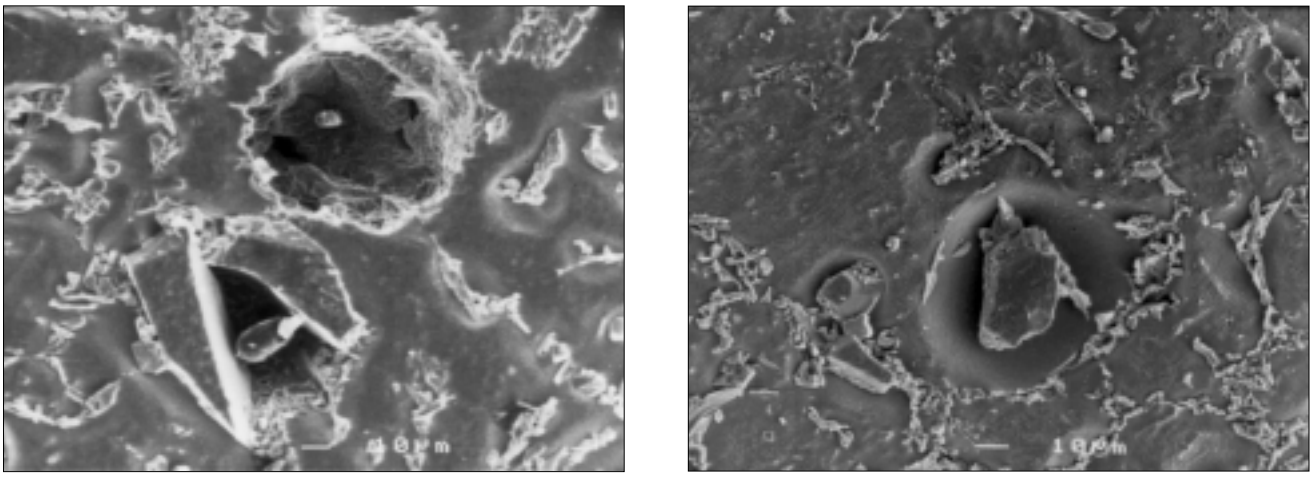

(a) (b)

FIGURE 7. *SEM micrographs of: (a) CA-05-20 composite and (b) CC-05-50 composite exposed to 3.5% NaCl for 28 days. (See Table 1 for composite characteristics.)*

❖ Pits were crystallographic in nature, and pits in the SiC composites were deeper than those in the Al_2O_3 composites. Microcrevice formation also was observed, possibly because of particle-matrix decohesion.

❖ Prolonged immersion tests revealed significant weight loss, mainly from corrosion of the matrix and from particle dropout. The overall weight loss in SiC composites was higher than in Al_2O_3 composites, which was attributable to differences in conductivity.

❖ Anodization and the application of ceria coatings to composites increased pitting resistance, probably through a reduction in the number of weak spots for initiation of pitting attack.

REFERENCES

1. P.P. Trzaskoma, E. McCafferty, C.R. Crowe, J. Electrochem. Soc. 130, 9 (1984): p. 1,804.
2. M. Metzger, S.G. Fishman, Ind. Eng. Chem. Prod. Res. Dev. 22, 2 (1983): p. 296.
3. D.M. Aylor, P.J. Moran, J. Electrochem. Soc. 132, 6 (1985): p. 1,277.
4. H. Sun, E.Y. Koo, H.G. Wheat, Corrosion 47, 10 (1991): p. 741.
5. K.A. Lucas, H. Clark, Corrosion of Al-Based MMCs (Somerset, England: Research Studies Press Ltd.,1993).
6. P.P. Trzaskoma, Metal-Matrix Composites: Mechanisms and Properties (San Diego, CA: Academic Press Inc.,1991).
7. K. Noda, H. Ono, T. Tsuru, H. Tezuka, A. Kamio, J. Japan Inst. Met. 56, 6 (1992): p. 641.
8. M.S.N. Bhat, M.K. Surappa, H.V.S. Naik, J. Mat. Sci. 26, 18 (1991): p. 4,991.
9. O.P. Modi, M. Saxena, B.K. Prasad, A.H. Yagneswaran, M.L. Vaidya, J. Mat. Sci. 27, 14 (1992): p. 3,897.
10. R.C. Paciej, V.S. Agarwala, Corrosion 44, 10 (1988): p. 680.
11. J.F. McIntyre, R.K. Conrad, S.L. Golledge, Corrosion 46, 11 (1990): p. 902.
12. T. Nishimura, Y. Simizu, M. Tamura, "Aluminum-Based Metal-Matrix Composites [MMC] Corrosion Performance," Proc. Conf. The Electrochem. Soc., Phoenix, Arizona, Oct. 14 ,1991 (Pennington, NJ: The Electrochemical Society, 1991).
13. D.J. Lloyd, H.P. Legace, A.D. McLeod, "Interfacial Phenomenon in Metal-Matrix Composites," in Controlled Interphases in Composite Materials, ICCI-IIT, ed. H. Ishida (Oxford, England: Elsevier Applied Science, 1990), p. 359.
14. A.J. Griffiths, A. Turnbull, NPL News, DMM (A) 31 (1992): p. 31.
15. S. Lin, H. Greene, H. Shih, F. Mansfeld, Corrosion 48, 1 (1992): p. 61.
16. F. Mansfeld, Y. Wang, H. Xiao, H. Shih, "Monitoring of Localized Corrosion of Aluminum Alloys with Electrochemical Impedance Spectroscopy [EIS]," Proc. Conf. Critical Factors in Localized Corrosion, Phoenix, Arizona, 1992 (Pennington, NJ: The Electrochemical Society, 1992), p. 469.
17. B.R.W. Hintoll, N.E. Ryan, D.R. Arnott, P.N. Trathan, L. Wilson, B.E. Williams, Corros. Australasia 10, 3 (1985): p. 12.
18. H. Ribes, M. Suery, G.L. Esperance, J.G. Legoux, Metall. T-A, 21A, 9 (1990): p. 2,489.
19. L.V. Ramanathan, "Effect of Liquid Metal Processing Parameters on Microstructure and Properties of Alumina-Reinforced Al-Based MMC," Proc. 12th Riso Int. Symp. Metal-Matrix Composites, eds. N. Hansen, D.J. Jensen, T. Leffers, H. Lilholt, T. Lorentzen, A.S. Pedersen, O.B. Pedersen, B. Ralph (Roskilde, Denmark: Riso National Laboratory, 1990), p. 611.
20. T. Lyman, "Appendix — Identification of Etchants," in Metals Handbook, 7th ed., vol. 7 (Metals Park, OH: ASM, 1972), p. 342.
21. "Microstructure of Aluminum Alloys," in Metals Handbook, 8th ed., vol. 7 (Metals Park, OH: ASM, 1972), p. 241.
22. F.A. Girot, L. Albingre, J.M. Quenisset, R. Naslain, J. Met. 11 (1987): p. 18.
23. D.J.A. Lloyd, Composites Sci. Technol. 35 (1989): p. 159.
24. E. Maahn, S. Roepstorff, "Corrosion Resistance of Aluminum-Silicon Carbide Composite Materials" Proc. 12th Riso Symp. Metal-Matrix Composites, eds. N. Hansen, D.J. Jensen, T. Leffers, H. Lilholt, T. Lorentzen, A.S. Pedersen, O.B. Pedersen, B. Ralph (Roskilde, Denmark: Riso National Laboratory, 1990), p. 497.
25. I.L. Muller, J.R. Galvele, Corros. Sci. 17 (1977): p. 179.
26. L.H. Hihara, R.M. Latanision, Corrosion 48, 7 (1992): p. 546.
27. W.W. Binger, E.H. Hollingsworth, D.O. Sprowls, "Resistance to Corrosion and Stress Corrosion," in Aluminum, vol. 1, Properties, Physical Metallurgy, and Phase Diagrams, ed. K.R. Van Horn (Metals Park, OH: ASM, 1967), p. 212.
28. P.P. Trzaskoma, Corrosion 46, 5 (1990): p. 402.
29. A. Turnbull, Brit. Corros. J. 27, 1 (1992): p. 27.
30. T.H. Nguyen, R.T. Foley, J. Electrochem. Soc. 126 (1979): p. 1,855.
31. R.T. Foley, Corrosion 42, 5 (1986): p. 277.
32. R. Stefac, F. Franz, Corros. Sci. 18 (1978): p. 16.
33. M. Shahid, G.E. Thompson, "Corrosion of Aluminum Alloy 8090/SiC Metal-Matrix Composites in NaCl and Na_2SO_4," Proc. Conf. Advanced Materials '91, Islamabad, Pakistan, Sept. 15, 1991.